Chemico-Biological Interactions 343 (2021) 109444

Contents lists available at ScienceDirect

Chemico-Biological Interactions

journal homepage: www.elsevier.com/locate/chembioint

Research paper

A new synthetic antitumor naphthoquinone induces ROS-mediated apoptosis with activation of the JNK and p38 signaling pathways

Patricia D.O. de Almeida [a], Gleyce dos Santos Barbosa Jobim [a], Caio César dos Santos Ferreira [a], Lucas Rocha Bernardes [a], Rosane B. Dias [b], Caroline B. Schlaepfer Sales [b,c], Ludmila de F. Valverde [b], Clarissa A.G. Rocha [b], Milena B.P. Soares [d], Daniel P. Bezerra [d], Fernando de Carvalho da Silva [e], Mariana Filomena do Carmo Cardoso [e], Vitor Francisco Ferreira [e], Larissa F. Brito [f], Lirlândia Pires de Sousa [f], Marne C. de Vasconcellos [a], Emerson S. Lima [a,*]

[a] Laboratory of Biological Activity, Faculty of Pharmaceutical Sciences, Federal University of Amazonas - UFAM, Manaus, Amazonas, 69077-000, Brazil
[b] Laboratory of Pathology and Molecular Biology, Gonçalo Moniz Institute, Oswaldo Cruz Foundation (IGM-FIOCRUZ/BA), Salvador, Bahia, 40296-710, Brazil
[c] Department of Biomorphology, Institute of Health Sciences, Federal University of Bahia - UFBA, Salvador, Bahia, 40110-902, Brazil
[d] Laboratory of Tissue Engineering and Immunopharmacology, Gonçalo Moniz Institute, Oswaldo Cruz Foundation (IGM-FIOCRUZ/BA), Salvador, Bahia, 40296-710, Brazil
[e] Laboratory of Carbohydrate and Nucleotide Synthesis, Department of Organic Chemistry, Federal Fluminense University – UFF, Niterói, Rio de Janeiro, 24020-141, Brazil
[f] Laboratory of Signaling in Inflammation, Department of Clinical and Toxicological Analysis, Faculty of Pharmacy, Federal University of Minas Gerais – UFMG, Belo Horizonte, Minas Gerais, 31270-901, Brazil

ARTICLE INFO

Keywords:
Naphthoquinone
Lawsone
Apoptosis
Anticancer drugs
Carcinogenesis
Breast cancer

ABSTRACT

Quinones are plant-derived secondary metabolites that present diverse pharmacological properties, including antibacterial, antifungal, antiviral, anti-inflammatory, antipyretic and anticancer activities. In the present study, we evaluated the cytotoxic effect of a new naphthoquinone 6b,7-dihydro-5H-cyclopenta [*b*]naphtho [2,1-d] furan-5,6 (9aH)-dione) (CNFD) in different tumor cell lines. CNFD displayed cytotoxic activity against different tumor cell lines, especially in MCF-7 human breast adenocarcinoma cells, which showed IC_{50} values of 3.06 and 0.98 μM for 24 and 48 h incubation, respectively. In wound-healing migration assays, CNFD promoted inhibition of cell migration. We have found typical hallmarks of apoptosis, such as cell shrinkage, chromatin condensation, phosphatidylserine exposure, increase of caspases-9 and-3 activation, increase of internucleosomal DNA fragmentation without affecting the cell membrane permeabilization, increase of ROS production, and loss of mitochondrial membrane potential induced by CNFD. Moreover, gene expression experiments indicated that CNFD increased the expression of the genes CDKN1A, FOS, MAX, and RAC1 and decreased the levels of mRNA transcripts of several genes, including CCND1, CDK2, SOS1, RHOA, GRB2, EGFR and KRAS. The CNFD treatment of MCF-7 cells induced the phosphorylation of c-jun N-terminal kinase (JNK) and p38 mitogen-activated protein kinases (MAPKs) and inactivation of extracellular signal-regulated protein kinase 1/2 (ERK1/2). In a study using melanoma cells in a murine model *in vivo*, CNFD induced a potent anti-tumor activity. Herein, we describe, for the first time, the cytotoxicity and anti-tumor activity of CNFD and sequential mechanisms of apoptosis in MCF-7 cells. CNFD seems to be a promising candidate for anti-tumor therapy.

1. Introduction

Despite advances in the drug discovery field, cancer prevention and control still represent a challenge, due to the unique characteristics of each type of cancer, resistance mechanisms, and wide spectrum of side effects. Among the many natural and synthetic compounds explored by

* Corresponding author. Universidade Federal do Amazonas – UFAM, Faculdade de Ciências Farmacêuticas, Avenida General Rodrigo Octávio, 6200, Coroado I, 69077-000, Manaus, AM, Brazil.
E-mail address: eslima@ufam.edu.br (E.S. Lima).

https://doi.org/10.1016/j.cbi.2021.109444
Received 8 September 2020; Received in revised form 11 December 2020; Accepted 9 March 2021
Available online 30 April 2021

Table 1
Cytotoxic effect of 6b,7-dihydro-5H-cyclopenta [*b*]naphtho [2,1-d]furan-5,6 (9aH)-dione) (CNFD) against different cell lines after 24 and 48 h incubation.

Cell lines	Histotypes	IC_{50} (μM)			
		CNFD		Doxorubicin	
		24 h	48 h	24 h	48 h
HCT-116	Human colon carcinoma	3.13	3.01	3.32	1.00
		2.69–3.64	2.30–3.95	1.83–6.02	0.78–1.27
MCF-7	Human breast adenocarcinoma	3.06	0.98	1.97	1.39
		2.77–3.37	0.27–1.08	0.95–2.09	0.56–2.45
SK-MEL-19	Human melanoma	7.25	3.43	1.2	0.72
		5.48–9.61	3.14–3.75	0.84–1.69	0.51–1.01
SK-MEL-28	Human melanoma	2.28	3.04	2.13	0.27
		1.49–3.50	1.88–4.90	1.70–2.67	0.17–0.42
SK-MEL-103	Human melanoma	3.28	2.11	1.09	0.53
		2.15–5.01	1.63–2.73	0.33–3.52	0.35–0.80
MESA/Dx5	Human sarcoma	2.8	2.35	8.23	3.91
		2.26–3.47	1.98–2.75	6.67–10.16	3.56–4.39
B16F10	Murine melanoma	3.77	1.24	1.95	0.55
		3.09–4.61	0.92–1.68	1.71–2.22	0.29–1.05
MRC-5	Human lung fibroblast	4.39	3.44	3.90	1.00
		2.64–7.31	3.13–3.77	3.15–4.83	0.59–1.71

Data are presented as IC_{50} values, in μM, and their 95% confidence interval obtained by nonlinear regression from two independent experiments performed in triplicate measured by the alamar blue assay after 24 h and 48 h incubation. Doxorubicin was used as the positive control.

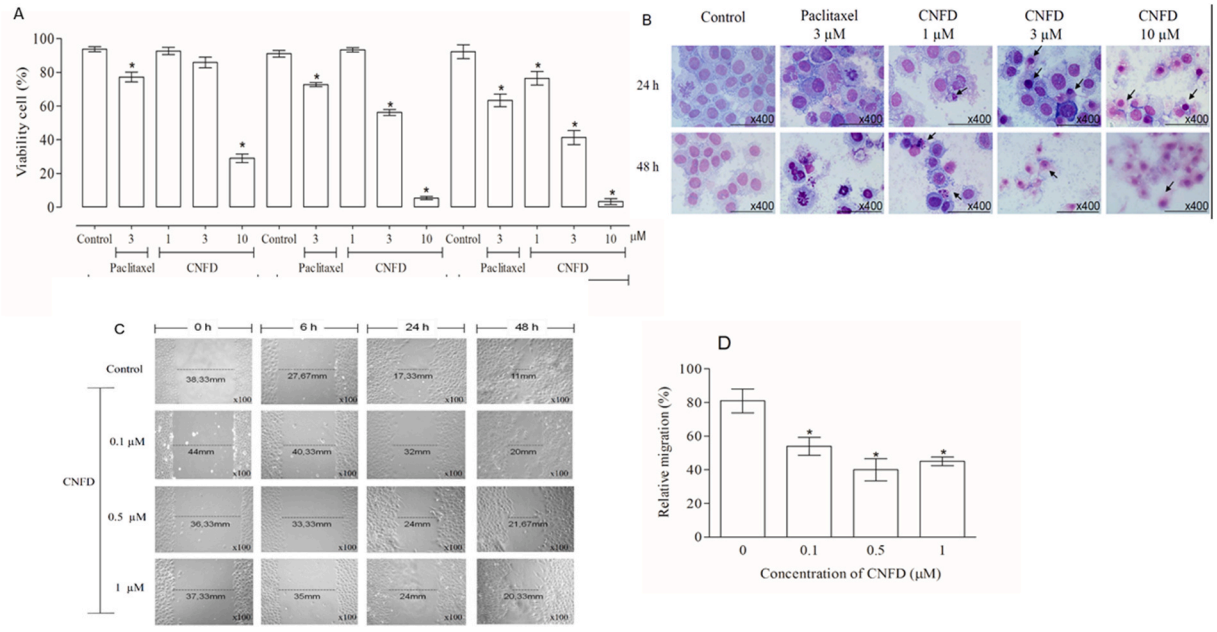

Fig. 1. Effect of 6b,7-dihydro-5H-cyclopenta [*b*]naphtho [2,1-d]furan-5,6 (9aH)-dione) (CNFD) on viability/morphology/motility of MCF-7 human breast adenocarcinoma cells. (A) Cell viability determined by trypan blue dye exclusion method after 12, 24 and 48 h incubation. (B) The cells were stained with hematoxylin–eosin and analyzed by optical microscopy after 24 h and 48 h incubation with CNFD at different concentrations. Negative control was treated with the vehicle (0.2% DMSO) used for diluting the substance tested. Paclitaxel (3 μM) was used as the positive control. (C) Wound healing assay was performed to evaluate the migration potential of MCF-7 cells after treatment with CNFD. (D) The relative migration of each sample was calculated from the difference in area of unclosed wound region measured between 0 and 48 h as compared to those of untreated control. Data are presented as mean values ± S.E.M. from three independent experiments performed in duplicate. *$p < 0.05$ compared to negative control by ANOVA followed by Student-Newman-Keuls test.

their anticancer potential, compounds containing quinone moieties have aroused interest in investigations [1,2].

Quinones are biologically active compounds found throughout nature. Naphthoquinone and its derivatives have a variety of biological responses, which include antiallergic, antibacterial, antifungal, anti-inflammatory, antithrombotic, antiplatelet, antiviral, antipyretic and anticancer properties [3]. The general mechanism of quinone toxicity may be correlated with the chemical behaviors of these compounds, such as redox cycling, arylation, interleaving, induction of DNA breaks and generation of free radicals [4–7]. Alternatively, reactive oxygen species (ROS) can activate a number of signaling pathways and are mediators of apoptosis via mitochondria-dependent mechanisms. In this context, the generation of ROS into the mitochondria, which occurs during quinone redox cycling, modifies membrane permeability, resulting in mitochondrial depolarization, Bax relocalization, cytochrome *c* release and caspase activation [8,9].

Previous studies have shown that the mitogen-activated protein kinases (MAPKs) pathways are critical in to convey diverse extracellular signals to biological responses, including ROS, and they modulate many cellular processes, such as cell proliferation, differentiation, and apoptosis [10]. Activated MAPKs play key roles in the activation of transcription factors and downstream kinases, leading to the induction

Table 2
Effect of 6b,7-dihydro-5H-cyclopenta [*b*]naphtho [2,1-d]furan-5,6 (9aH)-dione) (CNFD) on the DNA distribution of MCF-7 human breast adenocarcinoma cells after 24 h and 48 h incubation.

Treatment	Concentration (μM)	DNA distribution (%)			
		sub-G_1	G_0/G_1	S	G_2/M
After 24 h incubation					
Negative control	0.2% DMSO	0.4 ± 0.44	42.2 ± 2.16	42.5 ± 0.11	14.9 ± 1.78
Paclitaxel	3	25.3 ± 2.31*	13.3 ± 1.30*	4.8 ± 1.54*	56.6 ± 3.51*
CNFD	1	41.2 ± 0.97*	12.8 ± 0.38*	31.7 ± 1.12	14.4 ± 1.61
	3	38.0 ± 0.69*	10.8 ± 1.5*	35.0 ± 0.82	16.3 ± 1.01
	10	69.3 ± 2.10*	13.5 ± 1.66*	3.2 ± 1.77*	14.0 ± 2.0
After 48 h incubation					
Negative control	0.2% DMSO	9.7 ± 1.36	36.6 ± 5.32	27.7 ± 8.61	26.0 ± 4.65
Paclitaxel	3	9.5 ± 1.67	14.0 ± 1.65*	1.1 ± 0.98*	75.4 ± 4.03*
CNFD	1	35.6 ± 8.04*	25.2 ± 0.96*	23.6 ± 2.76	15.6 ± 4.78*
	3	63.7 ± 4.77*	20.0 ± 7.20*	8.2 ± 5.22*	8.1 ± 2.80*
	10	72.2 ± 8.81*	10.9 ± 5.31*	2.8 ± 2.42*	14.2 ± 6.13*

Data are presented as mean values ± S.E.M. from three independent experiments performed in duplicate. Negative control was treated with the vehicle used for diluting the substance tested. Paclitaxel was used as the positive control. Ten thousand events were evaluated per experiment and cellular debris was omitted from the analysis. Each phase was calculated using Flowjo v.10 program. *$p < 0.05$ compared to negative control by ANOVA followed by Student-Newman-Keuls test.

of immediate-early gene expression and subsequent changes in other cellular processes [11]. MAPKs can be grouped into three subfamilies, specifically, extracellular signal-related kinases 1/2 (ERK1/2), c-jun N-terminal kinase (JNK) and p38 MAP kinase [12,13]. ERK1/2 behaves mainly as mitogen-activated and proliferation/differentiation factor, whereas JNK and p38 MAP kinase are mainly stress-activated proteins related to apoptotic cell death [14,15].

6b,7-dihydro-5H-cyclopenta [*b*]naphtho [2,1-d]furan-5,6 (9aH)-dione) (CNFD) is a furan naphthoquinone synthesized from 2-hydroxy-1,4-naphthoquinone (Lawsone). Previous studies showed that CNFD displays antifungal activity against dermatophytes and yeasts. Furthermore, CNFD showed no hemolytic activity or cytotoxicity in murine fibroblasts [16,17]. Although the reports demonstrate the antifungal activity exercised by CNFD, its anti-tumor potential was not previously investigated. In the current study, CNFD was found to induce cytotoxic effect in different tumor cell lines, including MCF-7 human breast adenocarcinoma cells in a concentration- and time-dependent manner. Furthermore, CNFD induced apoptotic cell death in MCF-7 cells. The results of the present study will provide a molecular basis for understanding the anticancer activity of CNFD.

2. Materials and methods

2.1. Synthesis of naphthoquinone

CNFD (purity > 90%) was synthesized and identified as previously described by Freire et al., [2010]. Briefly, the furan naphthoquinone was obtained by oxidative [3 + 2] cycloaddition of 2-hydroxy-1,4-naphthoquinone (Lawsone) to the alkene, mediated by cerium (IV) ammonium nitrate.

2.2. In vitro cytotoxic activity assay

2.2.1. Alamar blue assay

HCT-116 (human colon carcinoma), MCF-7 (human breast adenocarcinoma), SK-MEL 19, 28 and 103 (human melanoma), MES-SA/Dx5 (human sarcoma), B16F10 (murine melanoma), and MRC-5 (human lung fibroblast) cell lines obtained from the American Type Culture Collection (ATCC), were cultured in Dulbecco's Modified Eagle Medium (DMEM) (Gibco by Life Technologies), supplemented with 10% fetal bovine serum (FBS, Gibco by Life Technologies), 100 U/mL penicillin, and 100 μg/mL streptomycin (Gibco by Life Technologies) at 37 °C with 5% CO_2. An equal number of cells (5×10^3) were incubated in 96-well plates and treated with different concentrations of CNFD (0.156–10 μM) for 72 h. Cell growth was measured by alamar blue assay [18]. Stock solutions of CNFD were prepared in DMSO and diluted in cell culture medium, with non-cytotoxic concentration of DMSO (0.2%). Negative control received the vehicle that was used for diluting the compound tested (0.2% DMSO). Doxorubicin (purity >99%; Sigma-Aldrich) was used as the positive control (0.156–10 μM). The determination of the 50% inhibitory concentration (IC_{50}) was performed by nonlinear regression.

2.2.2. Trypan blue exclusion assay

MCF-7 cells were seeded (7×10^4 cells/mL) in the absence or presence of different concentrations of CNFD (1, 3 and 10 μM). After each incubation period (12, 24, and 48 h), growth curves were established. Analysis of cells that were excluded from trypan blue was counted using a Neubauer chamber. Negative control was treated with the DMSO (0.2%) used for diluting the substance tested. Paclitaxel (purity >97%; Sigma-Aldrich), clinically useful as a chemotherapeutic agent, was used as positive control at a concentration of 2 μM due its high cytotoxicity and its use to induce apoptosis with high reproducibility of the results.

2.3. Morphological analyses using hematoxylin–eosin staining

In order to evaluate the cellular morphology, cells were harvested, transferred to cytospin slides, fixed with methanol for 30s, and stained with hematoxylin–eosin. Morphological changes were analyzed by light microscopy (Eclipse Ni, Nikon) using NIS-Elements 4.30.01 software (Nikon).

2.4. Wound-healing assay

Wound-healing assay was performed as reported by Liang et al., [2007] [19]. Briefly, MCF-7 cells were seeded in 12-well plates (4×10^5 cells per well) and incubated overnight to allow the cells to adhere on the surface of the plate. After cells reached to 80% of confluence, a straight line was made, to create a scratch, on the confluent monolayer of cells using a 200-μL sterile pipette tip. In order to remove debris and smooth the edge of the scratch, the cells were washed with 2 mL serum-free DMEM. Then, the cells were treated with low concentrations of CNFD (0.1, 0.5, and 1 μM). Untreated cells were used as negative control. Images were taken at 0, 6, 24, and 48 h after the scratch, and captured at × 100 magnification using a light microscopy (Axiovert.A1, Carl Zeiss). The quantification of uncovered areas was carried out using Zen 2 software (Carl Zeiss).

2.5. Cell cycle distribution and internucleosomal DNA fragmentation analysis

MCF-7 cells were deprived of FBS for 24 h for cell cycle synchronization. After treatment with 1, 3, and 10 μM of CNFD for 24 and 48 h, the cells were harvested in a permeabilization solution containing 0.1% Triton X-100 (SigmaAldrich), 2 μg/mL propidium iodide (Sigma-Aldrich Chemical), 0.1% sodium citrate, and 100 μg/mL RNAse (Sigma-Aldrich). Also, the cells were incubated in the dark for 15 min at room

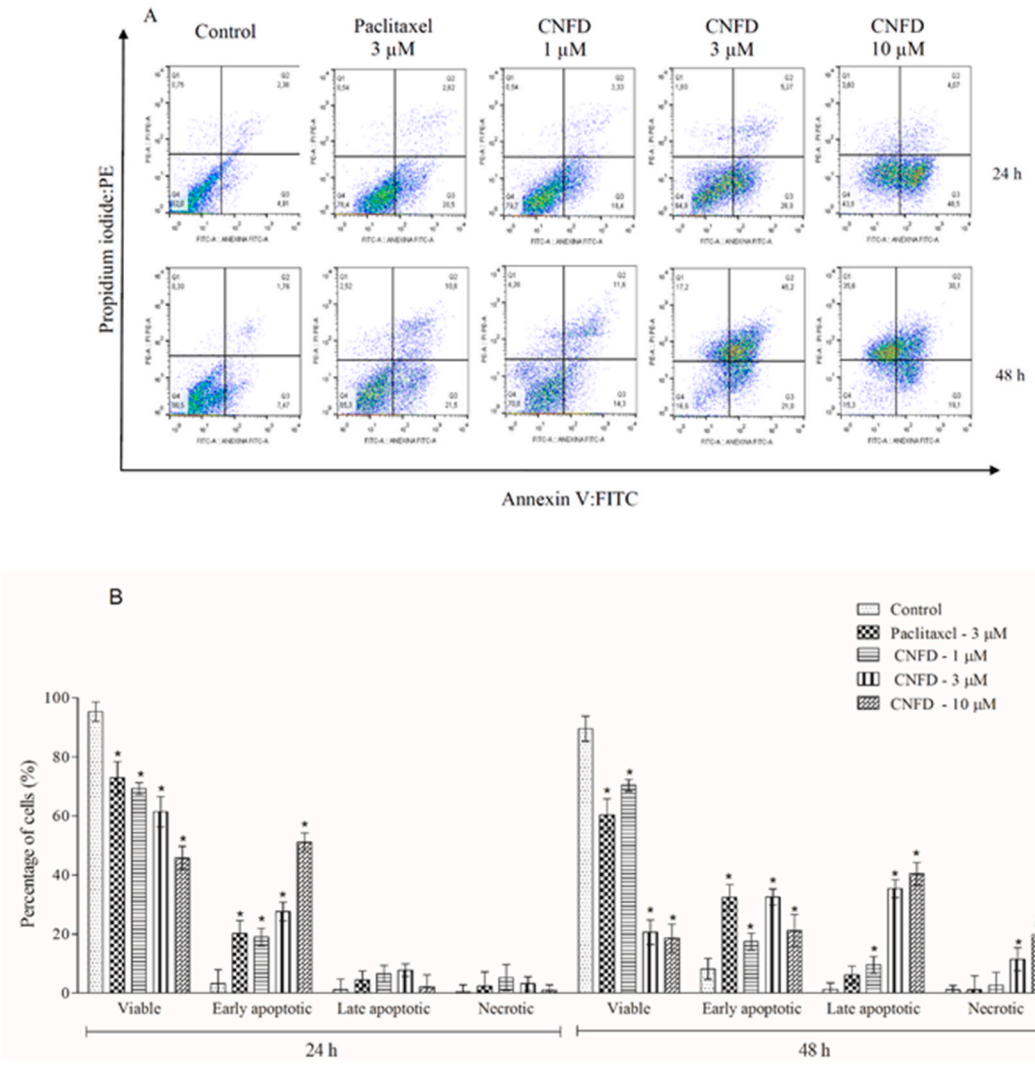

Fig. 2. Effect of 6b,7-dihydro-5H-cyclopenta [*b*]naphtho [2,1-d]furan-5,6 (9aH)-dione) (CNFD) in the induction of apoptosis in MCF-7 human breast adenocarcinoma cells. (A) Representative flow cytometric dot plots showing the percentage of cells in viable, early apoptotic, late apoptotic and necrotic stages. (B) Quantification of the cell viability determined by flow cytometry using annexin V/PI, after 24 h and 48 h incubation. Negative control was treated with the vehicle (0.2% DMSO) used for diluting the substance tested. Paclitaxel was used as the positive control. Ten thousand events were evaluated per experiment and cellular debris was omitted from the analysis. Data are presented as mean values ± S.E.M. from three independent experiments performed in duplicate. *$p < 0.05$ compared to negative control by ANOVA followed by Student-Newman-Keuls test.

temperature [20]. Finally, the cell fluorescence was determined by flow cytometry on a BD LSRFortessa cytometer (BD Biosciences) using the BD FACSDiva Software (BD Biosciences) and Flowjo Software 10 (Flowjo LCC).

2.6. Evaluation of apoptosis induction

For apoptosis detection, a FITC Annexin V Apoptosis Detection Kit I (BD Biosciences) was used. The analyses were performed according to the manufacturer's instructions. Briefly, the treated cells were collected after the indicated time, washed twice with cold PBS, and resuspended in 300 μL of binding buffer. Then, 5 μL of Annexin V-FITC staining buffer and 5 μL of propidium iodide were added to the cell suspension. The mixture was incubated in the dark at 37 °C for 15 min. Cell fluorescence was determined by flow cytometry on a BD LSRFortessa cytometer using BD FACSDiva Software and Flowjo Software 10.

2.7. Evaluation of caspases-8 and-9 activation

Caspase-8 and-9 activities were measured using colorimetric protease assay kits (Merck Millipore) according to the manufacturer's instructions. An aliquot of cell lysates (50 μL) was incubated with caspase-8 or caspase-9 substrate at 37 °C for 2 h. The samples were analyzed at 405 nm in SpectraMax 190, a microplate reader (Molecular Devices). The dosage of protein was performed in cell lysate using the Bradford method. The results were expressed as activity/mg protein.

2.8. Measurement of ROS production

ROS levels were measured according to previously described by Armstrong et al., [2002] [21] using 2′,7′-dichlorofluorescin diacetate (DCFDA) (Sigma-Aldrich). In brief, cells were treated with CNFD (1, 3, and 10 μM), hydrogen peroxide (500 μM), and paclitaxel (3 μM) for 3 h. Then, the cells were collected, washed with saline, and resuspended in FACS tubes with PBS containing 5 μM of DCFDA for 30 min. Finally, the cells were washed with saline and the cell fluorescence was determined by flow cytometry on a BD LSRFortessa cytometer using BD FACSDiva Software and Flowjo Software 10. Ten thousand events were evaluated per experiment and cellular debris was omitted from the analysis.

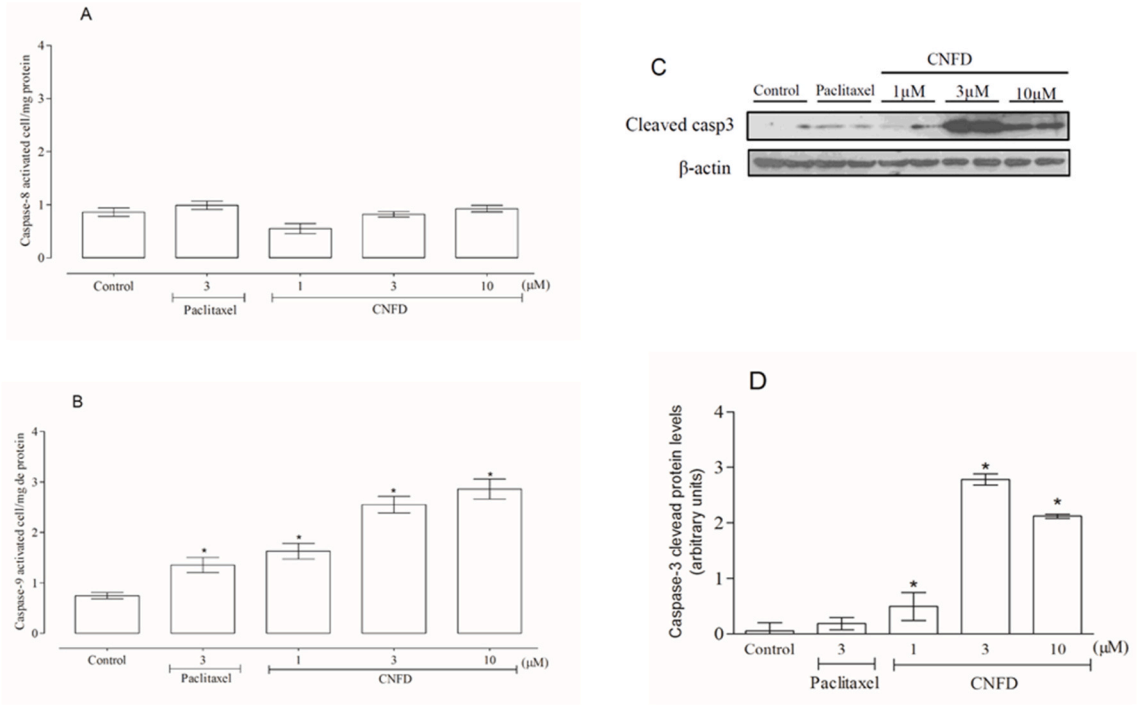

Fig. 3. Effect of 6b,7-dihydro-5H-cyclopenta [*b*]naphtho [2,1-d]furan-5,6 (9aH)-dione) (CNFD) on the activation of caspases in MCF-7 human breast adenocarcinoma cells (A–B) Activity of caspase 8 and caspase 9 determined by colorimetric protease assay kits. (C) Western blot analyses of caspase-3 cleaved from the whole cell lysates performed after CNFD and paclitaxel treatment for 24 h. (D) Responses (arbitrary units) of cleaved-caspase 3 and its respective beta-actin. Negative control was treated with the vehicle (0.2% DMSO) used for diluting the substance tested. Paclitaxel (3 μM) was used as the positive control. Data are presented as mean values ± S.E.M. from three independent experiments performed in duplicate. *$p < 0.05$ compared to negative control by ANOVA followed by Student-Newman-Keuls test.

2.9. *N-acetyl-L-cysteine (NAC) protection assay*

The protection assay using the antioxidant NAC was performed as described by Yedjou and Tchounwou [2007] [22]. In brief, prior to the viability assay, the cells were treated for 1 h with 10 mM NAC (Sigma-Aldrich), then incubated with CNFD in the established concentrations for 24 and 48 h. After, the cells were thoroughly trypsinized and the trypan blue exclusion assay was conducted as described above.

2.10. *Measurement of the mitochondrial transmembrane potential*

JC-1 is a sensitive fluorescent probe used as an indicator of mitochondrial potential in a variety of cell types. A mitochondrial depolarization was measured by MitoScreen JC-1 Kit (BD Biosciences) according to the manufacturer's instructions. MCF-7 cells were seeded in 24-well plates and treated with CNFD (1, 3 and 10 μM). After 24 h incubation, the culture medium was replaced by a medium containing 0.5 mL JC-1 dye and incubated for 15 min at 37 °C in the dark. Cell fluorescence was determined by flow cytometry on a BD LSRFortessa cytometer using BD FACSDiva Software and Flowjo Software 10. Ten thousand events were evaluated per experiment and cellular debris was omitted from the analysis.

2.11. *Gene expression analysis by PCR array*

MCF-7 cells were plated in culture bottles (7×10^4 cells/mL). After incubation for 12 h with CNFD 3 μM and paclitaxel, total RNA was isolated from the cells using RNeasy Plus mini kit (Qiagen) according to the manufacturer's instructions. The RNA was evaluated using a fluorimeter (QuBit™, Life Technologies). Reverse transcription of RNA was performed using Superscript VILO™ (Invitrogen Corporation). A 96-well plate, TaqMan® Array Human Molecular Mechanisms of Cancer (ID 4418806, Applied Biosystems™), was used for gene expression study by qPCR. The reactions were conducted on the ABI ViiA 7 (Applied Biosystems™). The conditions comprised a cycle at 50 °C for 2 min, at 95 °C for 20 s, then 40 cycles at 95 °C for 3 s, and at 60 °C for 30 s. The relative quantities (RQs) of mRNA expression were calculated by the ΔΔCT method (Livak and Schmittgen, 2001) using the Gene Expression Suite™ Software (Applied Biosystems™) and the cells were treated with the negative control (0.2% DMSO) as calibrator. The 18S and HPRT1 genes were used for gene expression normalization. All experiments were performed in DNase/RNase free conditions. The genes were considered to be upregulated if $RQ \geq 2$, which means that the gene expression in CNFD-treated cells was at least twice higher than the negative control-treated cells. Similarly, the genes were considered to be downregulated if $RQ \leq 0.5$, which means that the gene expression in CNFD-treated cells was half or less than half in comparison to the negative control-treated cells.

2.12. *Lysate preparation and western blot analysis*

Cells were lysed using the lysis buffer (50 mM tris-Cl, pH 8.0, 150 mM NaCl, 0,5% nonidet P-40,10% glycerol, 0.1 mM EDTA) in the presence of a mixture of protease and phosphatase inhibitors. Protein amounts were quantified with the Bradford assay reagent from Bio-Rad (Bio-Rad). Extracts (50 μg) were separated by electrophoresis on a denaturing 10–12% polyacrylamide-SDS gel and electrotransferred to nitrocellulose membranes. Membranes were blocked for 1 h with PBS containing 5% (w/v) nonfat dry milk and 0.1% tween 20, washed three times with PBS containing 0.1% tween 20 and, then, incubated with specific primary antibodies phospho-ERK1/2 (Thr202/Tyr204), phospho-p38 (Thr180/Tyr182), phospho-SAPK/JNK (Thr183/Tyr185), cleaved caspase-3 (Asp 175) and anti-β-actin (Cell Signaling Technology), using a dilution of 1:1000 in PBS buffer containing 5% (w/v) BSA and 0.1% tween 20. After washing, the membranes were incubated with appropriated HRP-conjugated secondary antibody (Cell

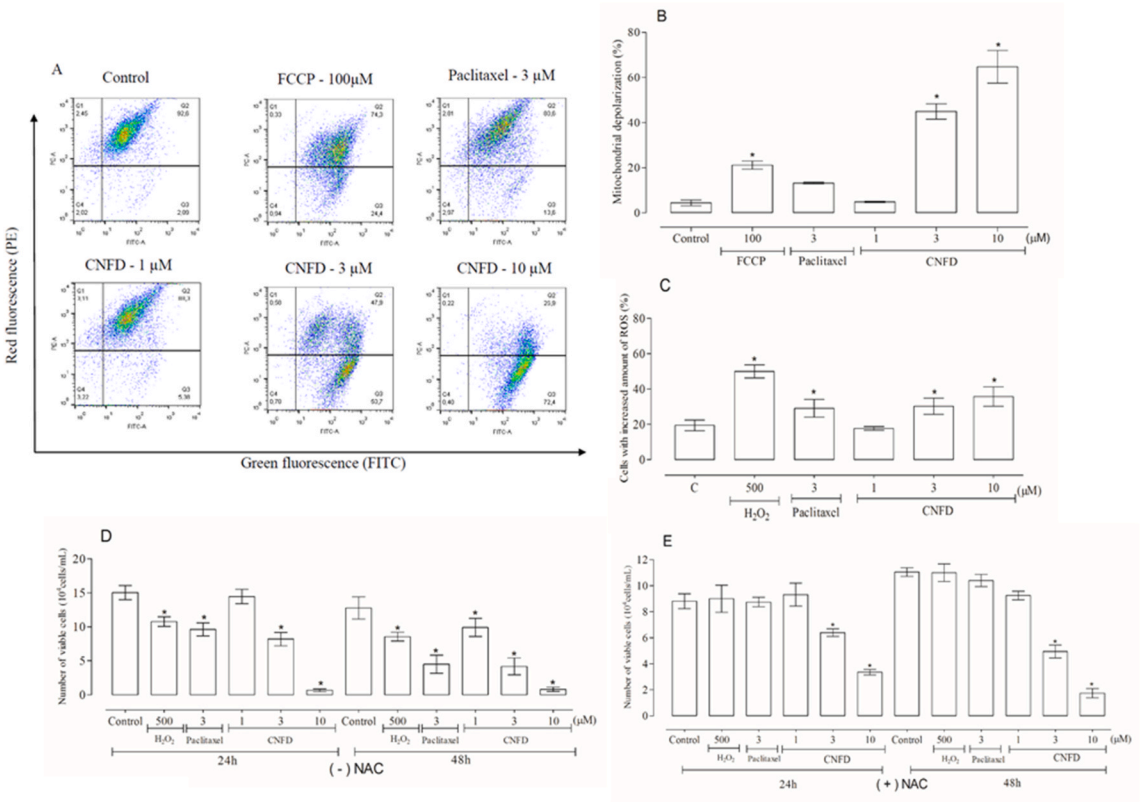

Fig. 4. Effect of 6b,7-dihydro-5H-cyclopenta [*b*]naphtho [2,1-d]furan-5,6 (9aH)-dione) (CNFD) on mitochondrial membrane potential and production of ROS in MCF-7 human breast adenocarcinoma cells. (A) Representative flow cytometric dot plots showing the percentage of mitochondrial depolarization. (B) Quantification of mitochondrial membrane potential determined by flow cytometry using JC-1 probe. Carbonilcyanide p-triflouromethoxyphenylhydrazone (FCCP, 100 μM), after 3 h of incubation, was used as the positive control. (C) ROS production measured by the DCFDA method. H_2O_2 (500 μM) was used as the positive control. (D) Cell viability determined by trypan blue dye exclusion method after 24 and 48 h incubation. (E) Viability cell after cotreatment with 10 mM of NAC for 60 min before the treatment of the CNFD at different concentrations for 24–48 h. Data are presented as mean values ± S.E.M. from three independent experiments performed in duplicate. For the flow cytometry experiments, ten thousand events were evaluated per experiment and cellular debris was omitted from the analysis. *$p < 0.05$ compared to negative control by ANOVA followed by Student-Newman-Keuls test.

Signaling Technology) (1:3000). Immunoreactive bands were visualized using ECL detection system, as described by the manufacturer (GE Healthcare) densitometry analyses.

2.13. Evaluation of anti-tumor activity

2.13.1. Animals

A total of 44 specific pathogen-free C57BL/6 mice (females, 20–30 g) were obtained and maintained at the animal facilities of Gonçalo Moniz Institute-FIOCRUZ/BA (Salvador, Bahia, Brazil). The animals were housed in cages with free access to food and water. All animals were kept under a 12:12 h light–dark cycle (lights on at 6:00 a.m.). The animals were treated according to the ethical principles for animal experimentation of SBCAL (Brazilian Association of Laboratory Animal Science), Brazil. The Animal Ethics Committee of Oswaldo Cruz Foundation (Salvador, Bahia, Brazil) approved the experimental protocol (number 001/2013).

2.13.2. Experimental protocol

The *in vivo* anti-tumor effect was evaluated in C57BL/6 mice. The animals were inoculated with B16–F10 melanoma as previously described by Costa et al., [2015] [23]. Tumor cells (2×10^6 cells per 500 μL) were implanted subcutaneously into the left hind groin of the mices. The animals were divided into five different groups: group 1 - animals that received injections of the vehicle (2% DMSO plus 2% kolifor in saline, negative control, n = 9); group 2 - animals that received injections of doxorubicin (0,5 mg/kg/day, positive control, n = 9); group 3 - animals that received injections of CNFD solution (10 mg/kg/day, n = 10); group 4 - animals that received injections of CNFD solution (30 mg/kg/day, n = 8); group 5- animals that received injections of CNFD solution (60 mg/kg/day, n = 8). The treatments were initiated one day after tumor injection. The animals were treated intraperitoneally (200 μL per animal) once daily for 13 consecutive days. Peripheral blood samples were collected from the retro-orbital plexus under anaesthesia for biochemical and haematological analysis on day 14, as described below. Animals were euthanized by cervical dislocation and tumors were excised and weighed. Drug effects were expressed as the percentage of inhibition in comparison to the negative control.

2.13.3. Systemic toxicological evaluation

Systemic toxicological effects were investigated as previously described by Costa et al., [2015]. The mice were weighed at the beginning and end of the experiment. The animals were observed whether there were signs of abnormalities throughout the study. Livers, kidneys, lungs, and hearts were removed, weighed, and examined for any signs of gross lesions or color changes and hemorrhage. Biochemical analyses of serum samples were performed using a Vet-16 rotor and quantified using an Analyst benchtop clinical chemistry system (Hemagen Diagnostics Inc.). Haematological analyses were performed using light microscopy. After macroscopic examination, tumors, livers, kidneys, lungs and hearts were fixed in 4% formalin buffer and embedded in paraffin. Tissue sections were stained with hematoxylin and eosin, and a pathologist performed the analysis under light

Table 3
The effect of 6b,7-dihydro-5H-cyclopenta [*b*]naphtho [2,1-d]furan-5,6 (9aH)-dione) (CNFD) on gene expression.

Gene symbol	Description	RQ	
		CNFD	Paclitaxel
Genes downregulated			
AKT1	AKT serine/threonine kinase 1	0.2360	0.2509
BCAR1	BCAR1, Cas family scaffolding protein	0.3289	0.1230
BCL2	BCL2, apoptosis regulator	0.0000	0.219
BID	BH3 interacting domain death agonist	0.2939	0.0000
CCND1	cyclin D1	0.3860	0.6869
CDK2	cyclin dependent kinase 2	0.4560	0.3919
CYCS	cytochrome *c*, somatic	0.0000	0.0000
DVL1	dishevelled segment polarity protein 1	0.2599	0.2890
E2F1	E2F transcription factor 1	0.3470	0.3740
EGFR	epidermal growth factor receptor	0.3580	0.4749
ELK1	ELK1, ETS transcription factor	0,424	0326
FADD	Fas associated via death domain	0,354	0.0000
FGF2	fibroblast growth factor 2	0,180	0.0000
FZD1	frizzled class receptor 1	0.1430	0.2240
GRB2	growth factor receptor bound protein 2	0.3070	0.3569
ITGAV	integrin subunit alpha V	0,359	0233
ITGB1	integrin subunit beta 1	0,447	0392
KRAS	KRAS proto-oncogene, GTPase	0.4839	0.3269
LEF1	lymphoid enhancer binding factor 1	0.3230	0.2049
MAP3K5	mitogen-activated protein kinase kinase kinase 5	0.2809	0.4230
MAPK1	mitogen-activated protein kinase 1	0.4530	0.3429
MAPK14	mitogen-activated protein kinase 14	0.1620	0.3330
MAPK3	mitogen-activated protein kinase 3	0.3000	0.1469
MDM2	MDM2 proto-oncogene	0.3659	0.4079
NRAS	Neuroblastoma RAS viral oncogene homolog	0.2310	0.8050
PIK3CA	phosphatidylinositol-4,5-bisphosphate 3-kinase catalytic subunit alpha	0.1850	0.2630
PIK3R1	phosphoinositide-3-kinase regulatory subunit 1	0.1729	0.4189
PTK2	protein tyrosine kinase 2	0.3050	0.5260
RHOA	ras homolog family member A	0.0000	0.0000
SOS1	SOS Ras/Rac guanine nucleotide exchange factor 1	0.4169	0.8700
TCF3	transcription factor 3	0.2259	0.2520
Genes upregulated			
CDKN1A	cyclin dependent kinase inhibitor 1A	3.0829	2.0539
FOS	Fos proto-oncogene, AP-1 transcription factor subunit	5.2459	1.7519
MAX	MYC associated factor X	3.2269	122,650.406
RAC1	ras-related C3 botulinum toxin substrate 1 (rho family, small GTP binding protein Rac1)	2.5859	1.0620

MCF-7 cells were treated with 3 μM of CNFD or paclitaxel for 12 h. After treatment, total RNA was isolated and reverse transcribed. Gene expression was detected using the TaqMan® Array Human Molecular Mechanisms of Cancer 96 plate. 18S e HPRT1 genes were used as endogenous gene for normalization. Values represent the relative quantitation (RQ) compared with the calibrator (negative control, 0.2% DMSO, RQ = 1.00). The genes were considered to be upregulated if RQ $\geq$ 2 and were considered to be downregulated if RQ $\leq$ 0.5.

microscopy.

2.14. Statistical analysis

Data are presented as mean ± SEM/SD or IC_{50} values and their 95% confidence intervals (CI 95%), which was obtained by nonlinear regression. Differences between experimental groups were compared using analysis of variance (ANOVA) followed by the Student–Newman–Keuls test ($p < 0.05$). All statistical analyses were performed using GraphPad (Intuitive Software for Science, San Diego, CA, USA).

3. Results

3.1. CNFD displayed cytotoxicity against different tumor cell lines

Several tumor cell lines were treated with increasing concentrations of CNFD for 24 and 48 h and analyzed by alamar blue assay. CNFD displayed cytotoxicity against all tumor cell lines, showing IC_{50} values in the micromolar range. Table 1 shows the IC_{50} values obtained. Doxorubicin was used as the positive control and also presented cytotoxicity against all tumor cell lines tested with IC_{50} values in the micromolar range. Similarly to doxorubicin, CNFD also showed cytotoxic effect against non-tumor cell line MRC-5. The selectivity indexes (SI) were 3.5 and 0.7 for CNFD and doxorubicin, respectively, after 48 h incubation (the SI was calculated using the following formula: SI=IC_{50} [MRC-5]/ IC_{50} [MCF-7]). Since MCF-7 cells were especially sensitive to the cytotoxic effect of CNFD, further studies were performed using this cell line.

We also evaluated cell viability by trypan blue dye exclusion method after 12, 24, and 48 h incubation, and it was observed that CNFD reduced the number of the viable cells after 12 h incubation ($p < 0.05$, Fig. 1A). After 24 and 48 h incubation, CNFD reduced the number of the viable cells in 45% and 95%; 58% and 98% at the concentrations of 3 and 10 μM, respectively ($p < 0.05$, Fig. 1A).

During morphological examination of the cells, severe drug-mediated changes were detected. CNFD-treated MCF-7 cells showed a morphology consistent with apoptosis in all concentrations tested (Fig. 1B), which included reduction in cell volume, chromatin condensation, and fragmentation of the nucleus. Paclitaxel also induced cell shrinkage, chromatin condensation and nuclear fragmentation, which displayed a morphology of apoptosis.

Furthermore, we demonstrated that CNFD was able to retard the migration of MCF-7 cells in the wound-healing assay. The ability of the cells to move and repopulate the wound region was suppressed by CNFD (Fig. 1C and D). At 0.5 μM, CNFD treatment reduced wound closure by 40% compared to untreated cells.

3.2. CNFD treatment causes internucleosomal DNA fragmentation in MCF-7 human breast adenocarcinoma cells

In order to further investigate the mechanisms involved in the cytotoxic activity of CNFD, its effect on the cell cycle progression was evaluated using flow cytometry. Table 2 shows the cell cycle distribution obtained. CNFD treatment, in all concentrations, resulted in a significant increase in the number of cells in sub-G_1 compared to the negative control ($p < 0.05$). In the control group, the percentages of cells corresponding to G_0/G_1 phases were 42.2 and 36.6%, to S phase were 42.5 and 27.7%, and to G_2/M phases were 14.9 and 26% at 24 and 48 h, respectively. Cells with internucleosomal DNA fragmentation (sub-G_1) corresponded to 0.4 and 9.7%, respectively, for the same times. For CNFD-treated cells, the percentages of cells corresponding to sub-G_1 were 41.2 and 35.6% (1 μM), 38 and 63.7% (3 μM), and 69.3 and 72.2% (10 μM) at 24 and 48 h, respectively, which corresponds to an increase in internucleosomal DNA fragmentation. Herein, paclitaxel led to cell cycle arrest in G_2/M phases.

3.3. CNFD treatment induces apoptosis in MCF-7 human breast adenocarcinoma cells

Externalization of phosphatidylserine on CNFD-treated cells was measured by flow cytometry using annexin V assay as well. In addition, propidium iodide staining was used to detect necrotic cells. CNFD treatment induced an increase of the percentage of apoptotic cells. As shown in Fig. 2A, CNFD induced apoptosis in a time-dependent manner ($p < 0.05$). The quantitative analysis showed the apoptosis rates (including early and late apoptosis), which were 38 and 60% after 24 h and 55 and 69% after 48 h of treatment, at the concentrations of 3 and 10 μM, respectively ($p < 0.05$, Fig. 2B).

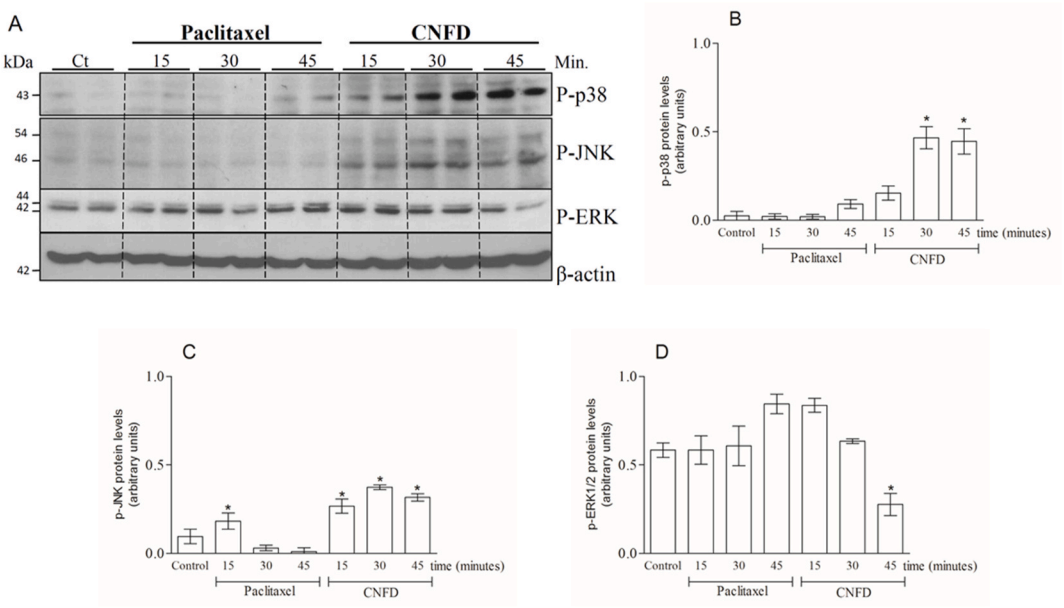

Fig. 5. Effect of 6b,7-dihydro-5H-cyclopenta [*b*]naphtho [2,1-d]furan-5,6 (9aH)-dione) (CNFD) on expression of phosphor-MAP kinases in MCF-7 cells. (A) Western blot analyses of phospho-p38, phospho-JNK and phospho-Erk1/2 from the whole cell lysates were performed after CNFD (3 μM) and Paclitaxel (3 μM) treatment indicated times. (B) Responses (arbitrary units) of phospho-p38 and its respective beta-actin. (C) Phospho-JNK and its respective beta-actin. (D) Phospho-ERK 1/2 and its respective beta-actin. Top: scanned image of one of three separate experiments. Bottom: semi-quantitative summary of three separate experiments using values obtained by densitometric analysis using Image J software. *$p < 0.05$ compared to negative control by ANOVA followed by Student-Newman-Keuls.

3.4. CNFD led apoptosis by mitochondrial pathway

In order to analyse the underlying mechanism of CNFD-induced apoptosis, we have examined the activation of caspases (caspases-8, -9 and-3) and the lost of mitochondrial transmembrane potential. Caspase-8 activation remained unchanged ($p > 0.05$, Fig. 3A); however, caspase-9 activation was increased in CNFD-treated cells ($p < 0.05$, Fig. 3B), suggesting the involvement of the intrinsic apoptosis pathway. Furthermore, it was observed an increased expression of cleaved caspase-3 ($p < 0.05$, Fig. 3C and D) after treatment with CNFD at concentrations of 3 and 10 μM. Additionally, CNFD induced mitochondrial depolarization in MCF-7 cells, as measured by JC-1 probe, suggesting intrinsic mitochondrial-dependent apoptosis (Fig. 4A). The mitochondrial depolarization occurred in 44 and 64% of the cells at concentrations of 3 and 10 μM, respectively ($p < 0.05$, Fig. 4 B).

In order to assess whether there is participation of ROS in CNFD-induced cell death, we evaluated ROS generation in MCF-7 cells. Treatment of MCF-7 cells with CNFD by 3 h promoted a concentration-dependent increase in ROS ($p < 0.05$, Fig. 4C). Interesting, cell death was prevented when the cells were co-treated with the antioxidant NAC ($p < 0.05$, Fig. 4D and E), enhancing cell survival in 18.0 and 12.1% (3 μM of CNFD), 33.7 and 9.4% (10 μM of CNFD) after treatment by 24 h and 48 h, respectively. Taken together, the data suggest that CNFD induces cytotoxic effects by the generation of oxidative radicals. However, this is not the only mechanism by which CNFD promotes cell death.

3.5. Effect of CNFD on gene expression

The effect of CNFD on the expression of genes involved in different cellular mechanisms, including cell proliferation, cell cycle, apoptosis, metastasis, and angiogenesis, was detected using TaqMan® Array Human Molecular Mechanisms of Cancer. Table 3 shows downregulated and upregulated genes in CNFD-treated MCF-7 cells. In the gene expression of cyclins (CCNDs), molecules that are involved in cell cycle progression [24], were observed downregulation of CCND1 (RQ = 0.386) after CNFD treatment, whereas the positive control, paclitaxel, was not able to reduce the expression of this gene (RQ = 0.687). In tumors, amplification and hyperactivation of cyclin dependent kinases (CDKs) are mechanisms that contribute to the dysregulation of the cell cycle, culminating in cell proliferation [25]. The treatments with CNFD and paclitaxel caused similar downregulation of CDK2 (CNFD RQ = 0.456; paclitaxel RQ = 0.392). Furthermore, cyclin dependent kinase inhibitor 1A (CDKN1A) was upregulated in CNFD-treated cells (RQ = 3.083), at higher extension than the paclitaxel treatment (RQ = 2.054).

MAPKs family play an important role in complex cellular programs such as proliferation, differentiation, development, transformation, and apoptosis [26]. Treatment with CNFD and paclitaxel reduced the expression of important oncogenes of this family, including MAPK1 (CNFD RQ = 0.453, paclitaxel RQ = 0.343), MAPK3 (CNFD RQ = 0.300, paclitaxel RQ = 0.147), MAPK14 (CNFD RQ = 0.162, paclitaxel RQ = 0.333), and MAP3K5 (CNFD RQ = 0.281; paclitaxel RQ = 0.423).

The RAS family is composed of oncoproteins GTPases, that participate in the regulation of pathways involved in cell growth and motility [27]. SOS1, a member of this family, was downregulated in cells treated with CNFD (RQ = 0.417), whereas paclitaxel did not alter the expression of this gene (RQ = 0.870). In addition, treatment with CNFD and paclitaxel inhibited the expression of the RHOA gene (CNFD RQ = 0.0; paclitaxel RQ = 0.0), which encodes a protein involved in cell motility.

The treatments with CNFD and paclitaxel also caused a sub regulation of genes related to the cell survival, as such AKT1 (CNFD RQ = 0.236; paclitaxel RQ = 0.251), PIK3R1 (CNFD RQ = 0.173; paclitaxel RQ = 0.419) and PIK3CA (CNFD RQ = 0.185, paclitaxel RQ = 0.263). Cells treated with CNFD showed lower expression of the anti-apoptotic gene BCL2 (RQ = 0.219), whereas no transcripts were detected for this gene after treatment with paclitaxel. However, the pro-apoptotic gene BID, a BCL2 antagonist, was downregulated in the cells treated with CNFD (RQ = 0.294) and was not detected in paclitaxel-treated cells.

CNFD treatment also induced upregulation of the genes FOS (RQ = 5.24) and MAX (RQ = 3.22). FOS gene is related to immediate response and quickly expressed [28], while MAX gene is capable of forming homodimers and heterodimers with family members, which include MAD, MXL1, and MYC, these transcriptionally active dimer can promote cell proliferation as well as apoptosis [29].

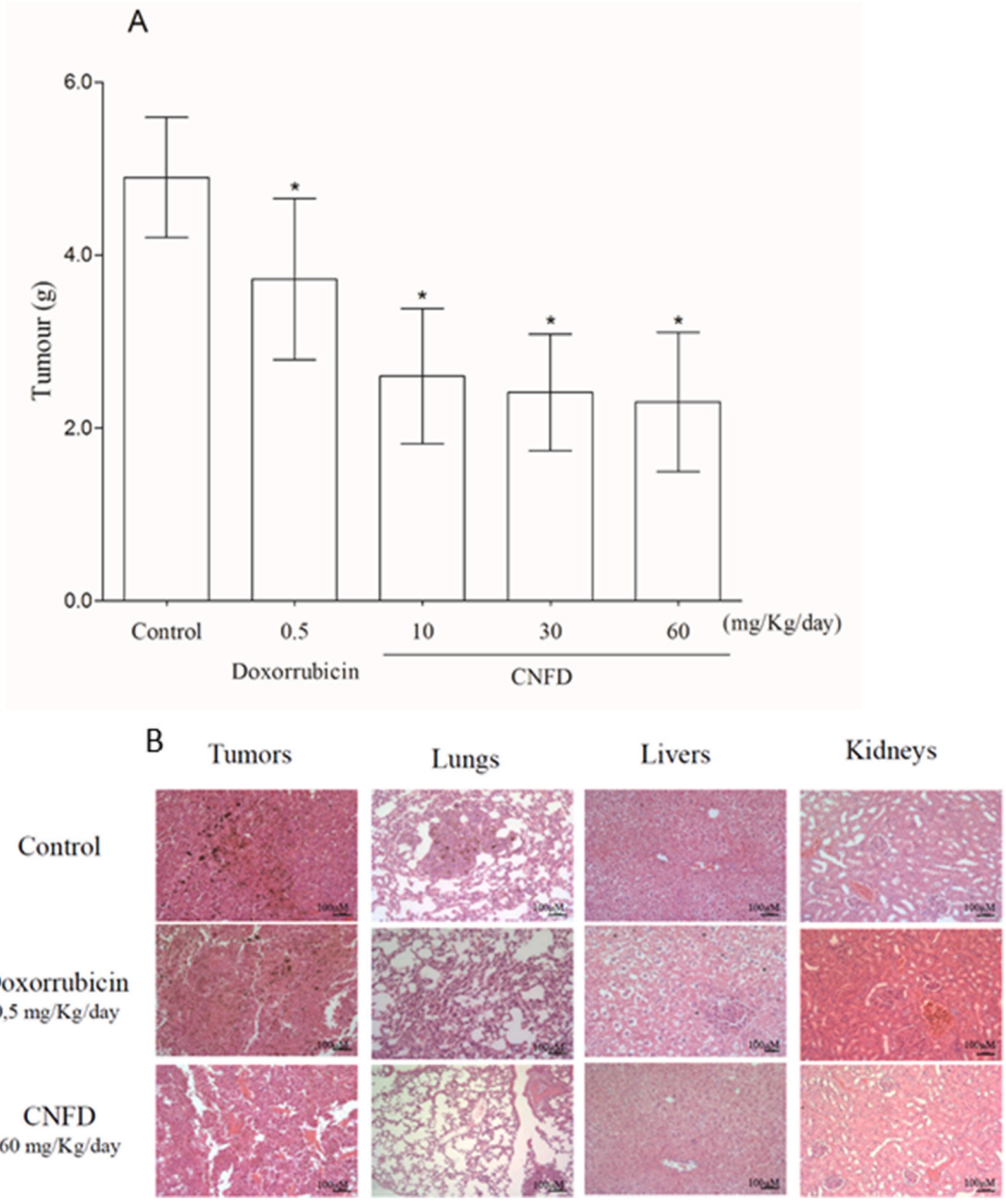

Fig. 6. *In vivo* anti-tumor effect of 6b,7-dihydro-5H-cyclopenta [*b*]naphtho [2,1-d]furan-5,6 (9aH)-dione) (CNFD). (A). Mice were injected with B16–F10 melanoma (2.0×10^6 cells/animal, s. c.). The animals received intraperitoneal drug administration for 13 consecutive days, beginning one day after tumor implantation. (B) Histopathology of excised tumors, lungs, liver and kidney of control and CNFD-treated mice. Representative photographs of H&E staining. Light microscopy magnification, 400x. Scale bar 100 μm. Doxorubicin (0.5 mg/kg/day) was used as the positive control. Negative control (control) were treated with the vehicle used for diluting the substance tested (2% DMSO plus 2% Kolifor in saline). Data are presented as the mean ± S.E.M. of 8–10 animals. *$p < 0.05$ compared to the negative control group using ANOVA followed by Student-Newman-Keuls test.

3.6. CNFD induces the activation of JNK and p-38 MAPK signaling pathways

Subsequently, we explored the upstream signaling pathways involved in CNFD-induced apoptosis. ERK1/2 is preferentially activated by growth factors, whereas c-jun NH2-terminal protein kinase (JNK) and p38 MAPK are preferentially activated by cell stress-inducing signals, such as oxidative stress, environmental stress and toxic chemical insults [11]. Thus, we queried whether CNFD-mediated apoptosis would be regulated by stress-activated protein kinases, JNK or p38 MAP kinase. We determined the effect of CNFD on the phosphorylation (as a measurement of activation) of the JNK, p38 and ERK1/2 MAPKs (Fig. 5A). Phosphorylation of JNK and p38 in CNFD-treated MCF-7 cells by a short time (15–45 min) showed a significant difference compared to untreated MCF-7 cells. The increase in phospho-p38 and phospho-JNK protein levels in MCF-7 cell treated with CNFD peaked at 30–45 min post-treatment ($p < 0.05$, Fig. 5B and C), afterwards the phosphorylation levels decreased gradually (data not shown). On the other hand, it was observed ERK inactivation at 45 min after CNFD treatment ($p < 0.05$ Fig. 5D). Thus, the results showed that exposure of MCF-7 cells to CNFD resulted in rapid activation of both JNK and p38 signaling and decreased ERK1/2 pathway.

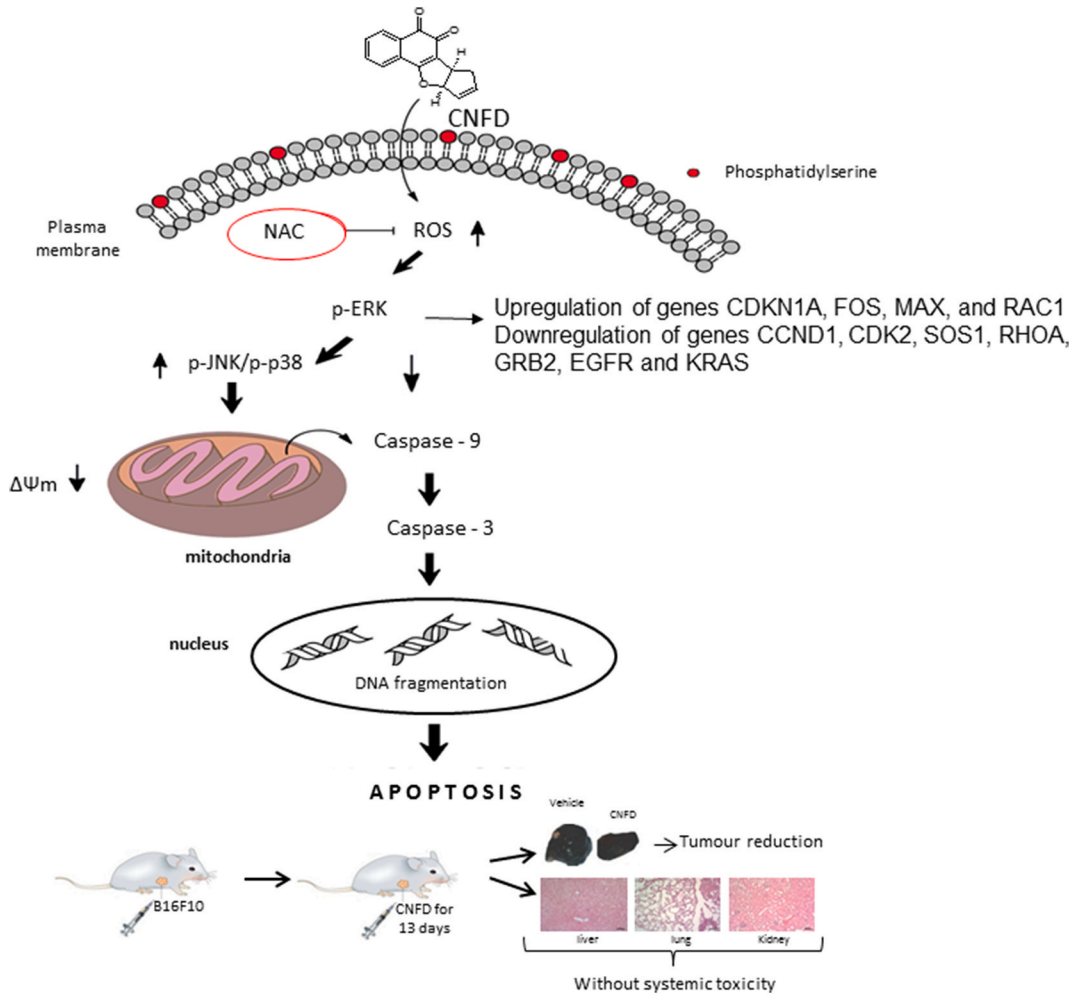

Fig. 7. The proposed mechanism of the action of 6b,7-dihydro-5H-cyclopenta [*b*]naphtho [2,1-d]furan-5,6 (9aH)-dione) (CNFD). CNFD promoted cell death by apoptosis with possible involvement of the intrinsic pathway and activating JNK and p38 MAPKs.

Table 4
Effect of CNFD on hematological parameters of peripheral blood from mice inoculated with B16F10 cells.

Treatment	Dosage (mg/Kg/day)	*N*	Erythrocytes (10^6 cell/μL)	Total leukocytes (10^3 cell/μL)	Differential leukocyte count (%)				
					Basophils	Eosinophils	Neutrophils	Lymphocytes	Monocytes
Vehicle	–	9	4,06 ± 0,80	2,70 ± 2,03	0,0 ± 0,0	0,2 ± 0,44	25,8 ± 4,26	71,6 ± 2,60	2,4 ± 2,50
Doxorubicin	0,5	9	2,73 ± 0,57*	2,96 ± 1,02	0,0 ± 0,0	0,0 ± 0,0	27,6 ± 5,54	71,6 ± 6,54	0,8 ± 1,09
CNFD	10	10	3,72 ± 1,56	2,34 ± 5,53	0,0 ± 0,0	0,2 ± 0,44	27,0 ± 6,28	68,8 ± 6,76	4,0 ± 1,87
CNFD	30	8	3,67 ± 2,27	2,44 ± 6,69	0,0 ± 0,0	0,0 ± 0,0	31,0 ± 9,84	67,6 ± 10,06	1,4 ± 2,60
CNFD	60	8	3,60 ± 0,82	3,35 ± 1,73	0,0 ± 0,0	0,2 ± 0,44	29,0 ± 13,3	66,8 ± 10,8	4,0 ± 2,0

The values correspond to the mean ± standard deviation. The negative control was treated with the vehicle (saline + DMSO 2% + Koliffor 2%) used to solubilize and dilute the test substances. Doxorubicin was used as a positive control. *$p < 0.05$ when compared to the negative control group by ANOVA (analysis of variance) followed by Student Newman-Keuls.

3.7. CNFD inhibits tumor growth in murine model of experimental melanoma

C57BL/6 mice were subcutaneously inoculated with B16–F10 melanoma cells and treated (intraperitoneally) daily for 13 consecutive days with CNFD to investigate its anti-tumor activity ($p < 0.05$, Fig. 7A). *In vivo* tumor growth was inhibited by the treatment with the CNFD (inhibition of 46, 50, and 52% at doses of 10, 30 and 60 mg/kg/day, respectively). The positive control, doxorubicin, at the dose of 0.5 mg/kg/day inhibited the tumor growth by 24%. Fig. 6B shows histopathological analyses of the excised tumors from all experimental groups that showed typical tumoral proliferation, consisting of round and oval cells, intense pleomorphism, large nuclei, irregular or multiple nucleoli, and atypical mitoses. Some of these neoplastic cells also presented intracellular melanin pigment. The stroma was scarce but displayed many areas of congested vessels and inflammation. In all groups, muscle invasion was observed. In CNFD (10, 30 and 60 mg/kg/day) and doxorubicin treated groups, extensive tumor necrosis, inflammation and even microabcession areas were visualized. In addition, in the CNFD (60 mg/kg/day) group, the tumor cells were well organized, and the tumor was more delimited. Systemic toxicological parameters were also examined in CNFD-treated mice. No significant changes in body or organ weight (liver, kidney, lung, and heart) were observed in CNFD-treated groups ($p > 0.05$, data not shown). No significant changes in peripheral blood

biochemistry ($p > 0.05$, data not shown) and as shown in Table 4, no changes in hematological parameters were observed in the groups treated with CNFD. Histopathological analyses of livers revealed an architectural disruption in all livers analyzed, including dilatation of vessels that make up the portal system. Other well-known and frequent findings were: centrilobular coagulative necrosis, congestion, inflammation and hydropic degeneration. In the groups treated with CNFD (10, 30, and 60 mg/kg/day) the histological changes (necrosis, inflammation, congestion) were less evident when compared to the positive and negative controls (Fig. 6B). There was no difference between the negative control group, doxorubicin, and CNFD (10, 30 and 60 mg/kg/day) in the kidneys. The changes described in this organ were: focal congestion, hemorrhage, glomerular sclerosis, tubular dilatation, focal inflammation, and vacuolization of tubular epithelial cells, and glomerular and tubular necrosis. These characteristics were less pronounced in the doxorubicin and CNFD (10 mg/kg/day) groups (Fig. 6B). Atelectasis, focal hemorrhage, and vascular congestion were observed in the lungs of all animals. Histopathological analyses of hearts did not show alterations in any group (Fig. 6B). The histopathological features in this study (hydropic change, vascular congestion and focal areas of inflammation) are acute cellular responses to non-lethal treatment-related stimuli, and the injured cells may return to a homoeostatic state when the aggression ends.

4. Discussion

Natural quinones are effective anticancer compounds both *in vitro* and *in vivo* [30]. In this study, we investigated the anticancer potential of CNFD, a new naphthoquinone synthesized from Lawsone. CNFD dramatically inhibited the proliferation of seven cancer cell lines, particularly in MCF-7 cells with an IC_{50} of less than 1 μM. In contrast, CNFD exhibited less toxic effect against noncancerous cells. Besides that, the growth inhibitory effect of CNFD towards MCF-7 cells was rapid in a short period of time, as the viability of MCF-7 cells was significantly reduced after 12 h of CNFD exposure.

Apoptosis is a regulated process under the control of several signaling pathways, such as caspases and mitochondrial pathways. Moreover, apoptotic cell death pathways can include the extrinsic or death receptor pathway and the intrinsic or mitochondrial pathway [31,32]. In the present study, the apoptosis induced by CNFD was confirmed by phosphatidylserine externalization, internucleosomal DNA fragmentation without affecting the cell membrane permeabilization, and activation of the caspase-9 and-3. The intrinsic pathway is initiated with loss of membrane potential in mitochondria and, then, there is the release of cytochrome *c* from the mitochondria into the cytosol and binding to the adaptor protein Apaf-1 following activation of caspase-9, which is a caspase initiator of the intrinsic apoptosis pathway [33,34]. The loss of mitochondrial membrane potential and the activation of caspase-9 observed in our study suggest the involvement of intrinsic apoptosis pathway in cell death induced by CNFD.

CNFD increases intracellular ROS, suggesting that ROS accumulation contributes to CNFD-induced cytotoxicity. In addition, the effect of CNFD on cell viability was partially protected by the antioxidant NAC, corroborating this hypothesis. As previously cited, quinone participates in a redox cycle, which reduces to hydroxynaphthoquinone and subsequently reduces the oxidation that generates ROS and, thus, it leads to oxidative stress [35]. The oxidative stress is considered an important condition to promote cell death in response to the activation of a number of signaling pathways as well as mediators of apoptosis by a mechanism dependent on mitochondria [36,37]. Indeed, quinones and naphthoquinones, including juglone, plubagin, shikonin and menadione have shown to promote the generation of ROS in other types of cell lines [38–41].

In addition to the mechanism of cell death induced by CNFD in MCF-7 cells mediated by ROS, we investigated the MAPK pathways. The family of MAPKs including ERK1/2, stress-activated protein kinase/c-jun N-terminal kinase (SAPK/JNK) and p38-MAPKs play central roles in signaling pathways of cell proliferation, survival and apoptosis [42]. ERK1/2 are activated by mitogens and growth factors leading to cell growth and survival, whereas JNK and p38 MAPK are preferentially activated by proinflammatory cytokines and oxidative stress resulting in cell differentiation and apoptosis [15,43,44]. In this study, we observed that JNK and p38 MAPK were phosphorylated, whereas the phosphorylation of ERK1/2 decreased after 30 min exposure with CNFD.

Gene expression experiment indicated that CNFD increased the expression of CDKN1A, FOS, MAX and RAC-1, and reduced the expression of BCL2, an apoptosis inhibitory gene. Constitutive expression of activated RAC induces activation of Jun N-terminal kinase (JNK), which phosphorylates and activates the transcription factor Jun [45]. The cellular genes c-FOS and c-JUN dimerize to form the transcription factor AP-1 (activator protein-1). These genes can be expressed minutes after drug exposure, chemical agents or growth factor deprivation, and the resulting products participate in several metabolic processes [46–49]. The MAX gene encodes a protein that interacts specifically with the Myc protein to form a heterodimer with high affinity for the specific cognate DNA binding site of Myc [50]. Our results corroborate with those of Kalra and co-workers [2004] [51], which found evidence that cFos is a mediator of the c-myc-induced apoptotic signaling via the p38 mitogen-activated protein kinase pathway.

The effect of CNFD on inhibition of migration in MCF-7 cells may be related to the downregulation of genes involved in RAS signaling such as SOS1, GRB2, and KRAS. SOS1 encodes a protein that exchanges guanine nucleotides and prepares the GTP binding site for Ras proteins that bind to the epidermal growth factor receptor (EGFR) pathway. Generally, stimulation in the EGFR pathway would initiate the activation of adapter proteins such as the SH-2 containing protein and the growth factor-2 receptor (GRB2) linked protein that recruits the SOS1 protein to the cell membrane. The association between GRB2 and SOS1 activates KRAS and further activates both RAF kinases, PI3Ks, MAPK and PI3K/AKT pathways, respectively [42,52]. The treatment with CNFD also caused downregulation of the AKT, PIK3, and MAPK family genes.

Furthermore, we observed upregulation of the RAC-1 gene and downregulation of RHOA, both of which are also involved in cell migration. RAC-1 drives oriented mesenchymal motility, leading edge protrusion and lamellipodia formation, and it is a key molecular player of regulated intracellular ROS sources. RHO activation is responsible for ameboid motility, a non-oriented movement which enables the cell to move between gaps of extracellular matrix instead of proteolytically degrade it [45,53]. The antagonistic effect on the regulation of RAC-1 and RHOA may be explained by the presence of ROS induced in the treatment of CNFD. Our studies continue to evaluate the possible antimetastatic effects induced by CNFD.

Evidence of cytotoxicity in a cell culture system is property possessed by most clinically used anti-tumor agents [54]. In addition to the cytotoxic effect of CNFD *in vitro*, this compound also demonstrated beneficial effects in a clinically relevant B16F10 murine melanoma model. CNFD showed significant reduction of tumor growth and tumor weight *in vivo* without significant effect in systemic toxicity. Regression of tumors in animals, growth reduction of sensitive tumors and/or increase in life expectancy are factors directly related to the antineoplastic activity [55]. The anticancer potential of naphthoquinones has also been determined in xenografts models *in vivo*, such as plumbagin, an extensively studied naphthoquinone, that it has been shown to exert significant anticancer potential in several animal models and *in vitro* protocols [56–59], including breast cancer [60–62].

In summary, our data showed that CNFD-mediated cytotoxicity is based on its ability to induce apoptosis (Fig. 7). Briefly, it occurs an increase of ROS production, loss of mitochondrial membrane potential, activation of caspase-9 and-3, internucleosomal DNA fragmentation, upregulation of the genes CDKN1A, FOS, MAX and RAC1, and downregulation of several genes, including CCND1, CDK2, SOS1, RHOA, GRB2, EGFR and KRAS, and activation of JNK and p38 MAPKs. These

results may provide sequential mechanisms of apoptosis induced by CNFD in MCF-7 cells.

Credit author statement

Patricia Almeida: Writing - Original Draft **Gleyce Jobim:** Investigation; Visualization **Caio Ferreira:** Investigation **Lucas Bernardes:** Formal analysis **Rosane Dias:** Investigation **Caroline Sales:** Methodology **Ludmila Valverde:** Investigation **Clarissa Rocha:** Methodology **Milena Soares:** Resources **Daniel Bezerra:** Methodology **Fernando Silva:** Validation **Mariana Cardoso:** Validation **Vitor Ferreira:** Resources **Larissa Brito:** Validation **Lirlândia Souza:** Resources **Marne Vasconcellos:** Supervision **Emerson Silva:** Project administration.

Data availability statement

The data that support the findings of this study are available from the corresponding author upon reasonable request.

Declaration of competing interest

The authors declare that they have no known competing financial interests or personal relationships that could have appeared to influence the work reported in this paper.

Acknowledgments

We wish to thank to Brazilian agencies CNPq, CAPES and FAPEAM for their financial support in the form of grants and fellowship awards. The authors thank to the histotechnology and flow cytometry platforms of FIOCRUZ-Bahia for the performance of histological techniques and flow cytometric data acquisition, respectively. The authors also thank to the Laboratory of Signaling in Inflammation from the Federal University of Minas Gerais (Belo Horizonte, Minas Gerais, Brazil) by technical assistance.

Appendix A. Supplementary data

Supplementary data to this article can be found online at https://doi.org/10.1016/j.cbi.2021.109444.

References

[1] D.B. Vendramini-costa, A. Alcaide, K.J. Pelizzaro-rocha, E. Talero, J. Ávila-román, R. Aloise, J. Ernesto, D. Carvalho, V. Motilva, Goniothalamin Prevents the Development of Chemically Induced and Spontaneous Colitis in Rodents and Induces Apoptosis in the HT-29 Human Colon Tumor Cell Line, vol. 300, 2016, pp. 1–12, https://doi.org/10.1016/j.taap.2016.03.009.

[2] M.R.S. Kumar, K. Aithal, B.N. Rao, N. Udupa, B.S.S. Rao, Cytotoxic, genotoxic and oxidative stress induced by 1,4-naphthoquinone in B16F1 melanoma tumor cells, Toxicol. Vitro 23 (2009) 242–250, https://doi.org/10.1016/j.tiv.2008.12.004.

[3] Y.M. Kanaan, J.R. Das, O. Bakare, N.M. Enwerem, S. Berhe, D. Beyene, V. Williams, Y.F. Zhou, R.L. Copeland, Biological evaluation of 2,3-dichloro-5,8-dimethoxy-1,4-naphthoquinone as an anti-breast cancer agent, Anticancer Res. 29 (2009) 191–199.

[4] X. Wang, B. Thomas, R. Sachdeva, L. Arterburn, L. Frye, P.G. Hatcher, D. G. Cornwell, J. Ma, Mechanism of arylating quinone toxicity involving Michael adduct formation and induction of endoplasmic reticulum stress, Proc. Natl. Acad. Sci. U.S.A. 103 (2006) 3604–3609, https://doi.org/10.1073/pnas.0510962103.

[5] E.A. Hillard, F.C. de Abreu, D.C.M. Ferreira, G. Jaouen, M.O.F. Goulart, C. Amatore, Electrochemical parameters and techniques in drug development, with an emphasis on quinones and related compounds, Chem. Commun. (2008) 2612–2628, https://doi.org/10.1039/b718116g.

[6] Y. Shang, C.Y. Chen, Y. Li, J.C. Zhao, T. Zhu, Hydroxyl radical generation mechanism during the redox cycling process of 1,4-naphthoquinone, Environ. Sci. Technol. 46 (2012) 2935–2942, https://doi.org/10.1021/es203032v.

[7] A.P. Neves, M.X.G. Pereira, E.J. Peterson, R. Kipping, M.D. Vargas, F.P. Silva jr., J. W.M. Carneiro, N.P. Farrell, Exploring the DNA binding/cleavage , cellular accumulation and topoisomerase inhibition of 2-hydroxy-3- (aminomethyl) -1 , 4-naphthoquinone Mannich bases and their platinum (II) complexes, J. Inorg. Biochem. 119 (2013) 54–64.

[8] K. Sinha, J. Das, P.B. Pal, P.C. Sil, Oxidative stress: the mitochondria-dependent and mitochondria-independent pathways of apoptosis, Arch. Toxicol. 87 (2013) 1157–1180, https://doi.org/10.1007/s00204-013-1034-4.

[9] J.D.B. Marinho-Filho, D.P. Bezerra, A.J. Araújo, R.C. Montenegro, C. Pessoa, J. C. Diniz, F.a. Viana, O.D.L. Pessoa, E.R. Silveira, M.O. de Moraes, L.V. Costa-Lotufo, Oxidative stress induction by (+)-cordiaquinone J triggers both mitochondria-dependent apoptosis and necrosis in leukemia cells, Chem. Biol. Interact. 183 (2010) 369–379, https://doi.org/10.1016/j.cbi.2009.11.030.

[10] Y. Son, Y.-K. Cheong, N.-H. Kim, H.-T. Chung, D.G. Kang, H.-O. Pae, Mitogen-activated protein kinases and reactive oxygen species: how can ROS activate MAPK pathways? J. Signal Transduct. 2011 (2011) 792639, https://doi.org/10.1155/2011/792639.

[11] X. Sui, N. Kong, L. Ye, W. Han, J. Zhou, Q. Zhang, C. He, H. Pan, P38 and JNK MAPK pathways control the balance of apoptosis and autophagy in response to chemotherapeutic agents, Canc. Lett. 344 (2014) 174–179, https://doi.org/10.1016/j.canlet.2013.11.019.

[12] L.C. Green, D. a Wagner, J. Glogowski, P.L. Skipper, J.S. Wishnok, S. R. Tannenbaum, Analysis of nitrate, nitrite, and [15N]nitrate in biological fluids, Anal. Biochem. 126 (1982) 131–138, https://doi.org/10.1016/0003-2697(82)90118-X.

[13] E.F. Wagner, Á.R. Nebreda, Signal integration by JNK and p38 MAPK pathways in cancer development, Nat. Rev. Canc. 9 (2009) 537–549, https://doi.org/10.1038/nrc2694.

[14] M. Cargnello, P.P. Roux, Activation and function of the MAPKs and their substrates, the MAPK-activated protein kinases, Microbiol. Mol. Biol. Rev. 75 (2011) 50–83, https://doi.org/10.1128/MMBR.00031-10.

[15] R.R. Jr, ERK1/2 MAP kinases : structure , function , and regulation, Pharmacol. Res. 66 (2012) 105–143, https://doi.org/10.1016/j.phrs.2012.04.005.

[16] C.P.V. Freire, S.B. Ferreira, N.S.M. de Oliveira, A.B.J. Matsuura, I.L. Gama, F.D. C. da Silva, M.C.B.V. de Souza, E.S. Lima, V.F. Ferreira, Synthesis and biological evaluation of substituted α- and β-2,3-dihydrofuran naphthoquinones as potent anticandidal agents, Medchemcomm 1 (2010) 229, https://doi.org/10.1039/c0md00074d.

[17] M.d. Ferreira, M.F.d.C. Cardoso, F.d.C. da Silva, V.F. Ferreira, E.S. Lima, J.V. B. Souza, Antifungal activity of synthetic naphthoquinones against dermatophytes and opportunistic fungi: preliminary mechanism-of-action tests, Ann. Clin. Microbiol. Antimicrob. 13 (2014) 26, https://doi.org/10.1186/1476-0711-13-26.

[18] S. a Ahmed, R.M. Gogal, J.E. Walsh, A new rapid and simple non-radioactive assay to monitor and determine the proliferation of lymphocytes: an alternative to [3H] thymidine incorporation assay, J. Immunol. Methods 170 (1994) 211–224, https://doi.org/10.1016/0022-1759(94)90396-4.

[19] C.C. Liang, A.Y. Park, J.L. Guan, In vitro scratch assay: a convenient and inexpensive method for analysis of cell migration in vitro, Nat. Protoc. 2 (2007) 329–333. https://doi.org/10.1038/nprot.2007.30.

[20] I. Nicoletti, G. Migliorati, M.C. Pagliacci, F. Grignani, C. Riccardi, A rapid and simple method for measuring thymocyte apoptosis by propidium iodide staining and flow-cytometry, J. Immunol. Methods 139 (1991) 271–279, https://doi.org/10.1016/0022-1759(91)90198-O.

[21] J.S. Armstrong, K.K. Steinauer, B. Hornung, J.M. Irish, P. Lecane, G.W. Birrell, D. M. Peehl, S.J. Knox, Role of glutathione depletion and reactive oxygen species generation in apoptotic signaling in a human B lymphoma cell line, Cell Death Differ. 9 (2002) 252–263, https://doi.org/10.1038/sj/cdd/4400959.

[22] C.G. Yedjou, P.B. Tchounwou, N-acetyl-L-cysteine affords protection against lead-induced cytotoxicity and oxidative stress in human liver carcinoma (HepG2) cells, Int. J. Environ. Res. Publ. Health 4 (2007) 132–137, https://doi.org/10.3390/ijerph2007040007.

[23] E.V. Costa, L.R.A. Menezes, S.L.A. Rocha, I.R.S. Baliza, R.B. Dias, A.G. Rocha, Clarissa, M.B.P. Soares, D.P. Bezerra, Antitumor properties of the leaf essential oil of zornia brasiliensis, Planta Med. (2015) 6.

[24] S. Lim, P. Kaldis, Cdks, cyclins and CKIs: roles beyond cell cycle regulation, Development 140 (2013) 3079–3093, https://doi.org/10.1242/dev.091744.

[25] M. Peyressatre, C. Prével, M. Pellerano, M.C. Morris, Targeting cyclin-dependent kinases in human cancers: from small molecules to peptide inhibitors, Cancers 7 (2015) 179–237, https://doi.org/10.3390/cancers7010179.

[26] W. Zhang, H.T. Liu, MAPK signal pathways in the regulation of cell proliferation in mammalian cells, Cell Res. 12 (2002) 9–18.

[27] E. Castellano, J. Downward, RAS interaction with PI3K: more than just another effector pathway, Genes Cancer 2 (2011) 261–274, https://doi.org/10.1177/1947601911408079.

[28] S. Bahrami, F. Drablos, Gene regulation in the immediate-early response process, Adv. Biol. Regul. 62 (2016) 37–49, https://doi.org/10.1016/j.jbior.2016.05.001.

[29] A. Banerjee, J. Hu, D.J. Goss, Thermodynamics of protein-protein interactions of cMyc, Max, and Mad: effect of polyions on protein dimerization, Biochemistry 45 (2006) 2333–2338, https://doi.org/10.1021/bi0522551.

[30] J.-J. Lu, J.-L. Bao, G.-S. Wu, W.-S. Xu, M.-Q. Huang, X.-P. Chen, Y.-T. Wang, Quinones derived from plant secondary metabolites as anti-cancer agents, Anticancer. Agents Med. Chem. 13 (2013) 456–463, https://doi.org/10.2174/187152013804910389.

[31] H.M. Korashy, Z.H. Maayah, A.R. Abd-Allah, A.O.S. El-Kadi, A.A. Alhaider, Camel milk triggers apoptotic signaling pathways in human hepatoma HepG2 and breast cancer MCF7 cell lines through transcriptional mechanism, J. Biomed. Biotechnol. 2012 (2012), https://doi.org/10.1155/2012/593195.

[32] S. Elmore, Apoptosis: a review of programmed cell death, Toxicol. Pathol. 35 (2007) 495–516, https://doi.org/10.1080/01926230701320337.

[33] S.W. Tait, D.R. Green, Mitochondria and cell death: outer membrane permeabilization and beyond, Nat. Rev. Cell Biol. 11 (2010) 621–632, https://doi.org/10.1038/nrm2952; 10.1038/nrm2952.
[34] I.R. Indran, G. Tufo, S. Pervaiz, C. Brenner, Recent advances in apoptosis, mitochondria and drug resistance in cancer cells, Biochim. Biophys. Acta Bioenerg. 1807 (2011) 735–745, https://doi.org/10.1016/j.bbabio.2011.03.010.
[35] K.W. Wellington, Understanding cancer and the anticancer activities of naphthoquinones – a review, RSC Adv. 5 (2015), https://doi.org/10.1039/C4RA13547D, 20309–20338.
[36] D. Bironaite, V.a. Kalvelyte, a Imbrasaite, a Stulpinas, The intracellular antioxidant balance of HL-60 cells and its implication in the apoptosis induced by quinoidal compounds, Biologija (2004) 48–51.
[37] C. Fleury, B. Mignotte, J.-L. Vayssière, Mitochondrial reactive oxygen species in cell death signaling, Biochimie 84 (2002) 131–141, https://doi.org/10.1016/S0300-9084(02)01369-X.
[38] V. Klaus, T. Hartmann, J. Gambini, P. Graf, W. Stahl, A. Hartwig, L.O. Klotz, 1,4-Naphthoquinones as inducers of oxidative damage and stress signaling in HaCaT human keratinocytes, Arch. Biochem. Biophys. 496 (2010) 93–100, https://doi.org/10.1016/j.abb.2010.02.002.
[39] L. Tian, D. Yin, Y. Ren, C. Gong, A. Chen, F.-J. Guo, Plumbagin induces apoptosis via the p53 pathway and generation of reactive oxygen species in human osteosarcoma cells, Mol. Med. Rep. 5 (2012) 126–132, https://doi.org/10.3892/mmr.2011.624.
[40] M.-J. Lee, S.-H. Kao, J.-E. Hunag, G.-T. Sheu, C.-W. Yeh, Y.-C. Hseu, C.-J. Wang, L.-S. Hsu, Shikonin time-dependently induced necrosis or apoptosis in gastric cancer cells via generation of reactive oxygen species, Chem. Biol. Interact. 211 (2014) 44–53, https://doi.org/10.1016/j.cbi.2014.01.008.
[41] D.N. Criddle, S. Gillies, H.K. Baumgartner-Wilson, M. Jaffar, E.C. Chinje, S. Passmore, M. Chvanov, S. Barrow, O.V. Gerasimenko, a.V. Tepikin, R. Sutton, O. H. Petersen, Menadione-induced reactive oxygen species generation via redox cycling promotes apoptosis of murine pancreatic acinar cells, J. Biol. Chem. 281 (2006) 40485–40492, https://doi.org/10.1074/jbc.M607704200.
[42] S.-H. Yang, A.D. Sharrocks, A.J. Whitmarsh, MAP kinase signalling cascades and transcriptional regulation, Gene 513 (2013) 1–13, https://doi.org/10.1016/j.gene.2012.10.033.
[43] F. Chen, JNK-induced apoptosis, compensatory growth, and cancer stem cells, Canc. Res. 72 (2012) 379–386, https://doi.org/10.1158/0008-5472.CAN-11-1982.
[44] T. Zarubin, J. Han, Activation and Signaling of the P38 MAP Kinase Pathway, vol. 15, 2005, pp. 11–18.
[45] M. Parri, P. Chiarugi, Rac and Rho GTPases in cancer cell motility control, Cell Commun. Signal. 8 (2010) 23, https://doi.org/10.1186/1478-811X-8-23.
[46] V. Appierto, M.G. Villani, E. Cavadini, R. Lotan, C. Vinson, F. Formelli, Involvement of c-Fos in fenretinide-induced apoptosis in human ovarian carcinoma cells, Cell Death Differ. 11 (2004) 270–279, https://doi.org/10.1038/sj.cdd.4401349.
[47] C. Lu, Q. Shen, E. DuPré, H. Kim, S. Hilsenbeck, P.H. Brown, cFos is critical for MCF-7 breast cancer cell growth, Oncogene 24 (2005) 6516–6524, https://doi.org/10.1038/sj.onc.1208905.
[48] S. Markopoulou, E. Kontargiris, C. Batsi, T. Tzavaras, I. Trougakos, D.A. Boothman, E.S. Gonos, E. Kolettas, Vanadium-induced apoptosis of HaCaT cells is mediated by c-fos and involves nuclear accumulation of clusterin, FEBS J. 276 (2009) 4208–4223, https://doi.org/10.1111/j.1742-4658.2009.07093.x.
[49] M. Santos, A. Tannuri, M. Coelho, J. Gonçalves, S. Serafini, L. Silva, U. Tannuri, Immediate expression of c-fos and c-jun mRNA in a model of intestinal autotransplantation and ischemia-reperfusion in situ, Clinics 70 (2015) 373–379, https://doi.org/10.6061/clinics/2015(05)12.
[50] B. Hoffman, D. a Liebermann, Apoptotic signaling by c-MYC, Oncogene 27 (2008) 6462–6472, https://doi.org/10.1038/onc.2008.312.
[51] N. Kalra, V. Kumar, c-Fos is a mediator of the c-Myc-induced apoptotic signaling in serum-deprived hepatoma cells via the p38 mitogen-activated protein kinase pathway, J. Biol. Chem. 279 (2004) 25313–25319, https://doi.org/10.1074/jbc.M400932200.
[52] E. Castellano, M. Molina-Arcas, A.A. Krygowska, P. East, P. Warne, A. Nicol, J. Downward, RAS signalling through PI3-Kinase controls cell migration via modulation of Reelin expression, Nat. Commun. 7 (2016) 1–112, https://doi.org/10.1038/pj.2016.37.
[53] M. Raftopoulou, A. Hall, Cell migration: rho GTPases lead the way, Dev. Biol. 265 (2004) 23–32, https://doi.org/10.1016/j.ydbio.2003.06.003.
[54] S. Rajasekar, D.J. Park, C. Park, S. Park, Y.H. Park, S.T. Kim, Y.H. Choi, Y.W. Choi, In vitro and in vivo anticancer effects of Lithospermum erythrorhizon extract on B16F10 murine melanoma, J. Ethnopharmacol. 144 (2012) 335–345, https://doi.org/10.1016/j.jep.2012.09.017.
[55] P.M.P. Ferreira, D.P. Bezerra, J. Do Nascimento Silva, M.P. Da Costa, J.R. De Oliveira Ferreira, N.M.N. Alencar, I.S.T. De Figueiredo, A.J. Cavalheiro, C.M. L. Machado, R. Chammas, A.P.N.N. Alves, M.O. De Moraes, C. Pessoa, Preclinical anticancer effectiveness of a fraction from Casearia sylvestris and its component Casearin X: in vivo and ex vivo methods and microscopy examinations, J. Ethnopharmacol. 186 (2016) 270–279, https://doi.org/10.1016/j.jep.2016.04.011.
[56] M.H. Aziz, N.E. Dreckschmidt, A.K. Verma, Plumbagin, a medicinal plant-derived naphthoquinone, is a novel inhibitor of the growth and invasion of hormone-refractory prostate cancer, Canc. Res. 68 (2008) 9024–9032, https://doi.org/10.1158/0008-5472.CAN-08-2494.
[57] A. Kawiak, J. Piosik, G. Stasilojc, A. Gwizdek-Wisniewska, L. Marczak, M. Stobiecki, J. Bigda, E. Lojkowska, Induction of apoptosis by plumbagin through reactive oxygen species-mediated inhibition of topoisomerase II, Toxicol. Appl. Pharmacol. 223 (2007) 267–276, https://doi.org/10.1016/j.taap.2007.05.018.
[58] M. Niu, W. Cai, H. Liu, Y. Chong, W. Hu, S. Gao, Q. Shi, X. Zhou, X. Liu, R. Yu, Plumbagin inhibits growth of gliomas in vivo via suppression of FOXM1 expression, J. Pharmacol. Sci. 128 (2015) 131–136, https://doi.org/10.1016/j.jphs.2015.06.005.
[59] D. Raghu, D. Karunagaran, Plumbagin downregulates wnt signaling independent of p53 in human colorectal cancer cells, J. Nat. Prod. 77 (2014) 1130–1134, https://doi.org/10.1021/np4010085.
[60] K.A. Manu, M.K. Shanmugam, P. Rajendran, F. Li, L. Ramachandran, H.S. Hay, R. Kannaiyan, S.N. Swamy, S. Vali, S. Kapoor, B. Ramesh, P. Bist, E.S. Koay, L.H. K. Lim, K.S. Ahn, A.P. Kumar, G. Sethi, Plumbagin inhibits invasion and migration of breast and gastric cancer cells by downregulating the expression of chemokine receptor CXCR4, Mol. Canc. 10 (2011) 107, https://doi.org/10.1186/1476-4598-10-107.
[61] B. Sung, B. Oyajobi, B.B. Aggarwal, Plumbagin inhibits osteoclastogenesis and reduces human breast cancer-induced osteolytic bone metastasis in mice through suppression of RANKL signaling, Mol. Canc. Therapeut. 11 (2012) 350–359, https://doi.org/10.1158/1535-7163.MCT-11-0731.
[62] A. Ahmad, S. Banerjee, Z. Wang, D. Kong, F.H. Sarkar, Plumbagin-induced apoptosis of human breast cancer cells is mediated by inactivation of NF-κB and Bcl-2, J. Cell. Biochem. 105 (2008) 1461–1471, https://doi.org/10.1002/jcb.21966.